https://doi.org/10.5194/amt-2020-341
Preprint. Discussion started: 9 November 2020

Atmospheric Measurement Techniques Discussions

Highly time-resolved characterization of carbonaceous aerosols using a two-wavelength Sunset thermo/optical carbon analyzer

Mengying Bao[1,2,3], Yan-Lin Zhang[1,2,3*], Fang Cao[1,2,3], Yu-Chi Lin[1,2,3], Yuhang Wang[4], Xiaoyan Liu[1,2,3], Wenqi Zhang[1,2,3], Meiyi Fan[1,2,3], Feng Xie[1,2,3], Robert Cary[5], Joshua Dixon[5] and Lihua Zhou[6]

1 Yale-NUIST Center on Atmospheric Environment, Joint International Research Laboratory of Climate and Environment Change (ILCEC), Nanjing University of Information Science and Technology, Nanjing 210044, China

2 Key Laboratory of Meteorological Disaster Ministry of Education (KLME), Collaborative Innovation Center on Forecast and Evaluation of Meteorological Disasters (CIC-FEMD), Nanjing University of Information Science and Technology, Nanjing 210044, China

3 School of Applied Meteorology, Nanjing University of Information Science and Technology, Nanjing 210044, China

4 School of Earth and Atmospheric Sciences, Georgia Institute of Technology, Atlanta 30332, USA

5 Sunset Laboratory, 1080 SW Nimbus Avenue, Suite J/5 Tigard, OR 97223, USA

6 College of Global Change and Earth System Science, Beijing Normal University, Beijing 100875, China

Correspondence: Yan-Lin Zhang (dryanlinzhang@outlook.com)

Abstract

Carbonaceous aerosols have great influence on the air quality, human health and climate change. Except for organic carbon (OC) and elemental carbon (EC), brown carbon (BrC), mainly originates from biomass burning, as a group of OC with strong absorption from the visible to near-ultraviolet wavelengths, makes a considerable contribution to global warming. Large amounts of studies have reported long-term observation of OC and EC concentrations throughout the word, but studies of BrC based on long-term observations are rather limited. In this study, we established a two-wavelength method (658 nm and 405 nm) applied in the Sunset thermo/optical carbon analyzer. Based on one-year observation, we firstly investigated the characteristics, meteorological impact and transport process of OC and EC. Due to BrC absorbs light at 405 nm more effectively

https://doi.org/10.5194/amt-2020-341
Preprint. Discussion started: 9 November 2020


Atmospheric Measurement Techniques Discussions

than 658 nm, we defined the enhanced concentrations (dEC =$EC_{405\ nm}$—$EC_{658\ nm}$) and gave the possibility to provide an indicator of BrC. The receptor model and MODIS fire information were used to identify the presence of BrC aerosols. Our results showed that the carbonaceous aerosols concentrations were highest in winter and lowest in summer. Traffic emission was an important source of carbonaceous aerosols in Nanjing. Receptor model results showed that strong local emissions were found in OC and EC aerosols, however dEC aerosols were significantly affected by regional or long-range transport. The dEC/OC and OC/EC ratios showed similar diurnal patterns and the dEC/OC increased when the OC/EC ratios increased, indicating strong secondary sources or biomass burning contributions to dEC. Two biomass burning events both in summer and winter were analyzed and the results showed that the dEC concentrations were obvious higher in biomass burning days, however, no similar levels of the OC and EC concentrations were found both in biomass burning days and normal days in summer, suggesting that biomass burning emission made a great contribution to dEC and the sources of OC and EC were more complicated. Large number of open fire counts from the northwest and southwest areas of the study site were monitored in winter, significantly contributed to OC, EC and dEC. In addition, the near-by YRD area was one of the main potential source areas of dEC, suggesting that anthropogenic emissions could also be important sources of dEC. The results proved that dEC can be an indicator of BrC in biomass burning days. Our modified two-wavelength instrument provided more information than traditional single-wavelength thermo/optical carbon analyzer and gave a new idea about the measurement of BrC, the application of dEC data need to be further investigated.

1. Introduction

Carbonaceous aerosols including orgainc carbon (OC) and elemental carbon (EC), which have significant influence on the global radiative transfer, human health and atmospheric visibility, have been the focus of research in the atmospheric environment field for many years (Lelieveld et al., 2015; Wu and Yu, 2016; Wang et al., 2018; Zhang et al., 2017; Liu et al., 2019; Zhang et al., 2019). EC mainly originates from fossil fuel and biomass combustion, and is estimated to be the second largest warming factor behind CO_2 contributing to climate change (Liu et al., 2015; Zhang and Kang, 2019; Cao and Zhang, 2015). OC originates both from primary emissions and gas-to-particle conversion as secondary organic carbon (SOC) and can scatter the solar radiation which causes negative forcing globally (Zhou et al., 2014; Huang et al., 2014).

https://doi.org/10.5194/amt-2020-341
Preprint. Discussion started: 9 November 2020


Atmospheric Measurement Techniques Discussions

In the recent decades, brown carbon (BrC), as a kind of light-absorbing organic carbon which can absorb light especially from near-UV to visible wavelength, has caused global concern due to its positive climate effect (Andreae and Gelencsér, 2006; Zhang et al., 2020). BrC is mainly emitted from anthropogenic and biogenic emissions (Zhang et al., 2011). Previous studies have proved that biomass burning and biofuel combustion are the most important sources of primary BrC (Saleh et al., 2014; Wu et al., 2020; Lei et al., 2018). Recent researches reported that in developing countries such as China and India, the contribution of fossil fuel combustion to BrC can't be ignored (Satish et al., 2017; Yan et al., 2017; Kirillova et al., 2014). Secondary BrC is mainly emitted from heterogeneous photo-oxidation reactions or aqueous reactions of anthropogenic and biogenic precursors (Zhang et al., 2020; Li et al., 2020; Zhang et al., 2011). However, due to the lack of understanding of BrC at the molecular level and in situ BrC data, there are still large uncertainties in the estimates of the distribution and the magnitude of BrC climate effect in both remote sensing and modeling method (Arola et al., 2011; Feng et al., 2013).

The thermo-optical analysis (TOA) method is one of the most widely used quantitative method of OC and EC taking use of the difference between the thermo-optical properties of OC and EC (Birch and Cary, 1996; Chow et al., 2004). OC and EC will be volatilized at different heating protocol. The reflectance/transmittance of one laser source (near-infrared wavelength) through the sample filter are continuously monitored and return of the reflectance/transmittance to its initial value on the thermograph was taken as a split point between OC and EC. This way, the formation of pyrolyzed carbon which can also absorb the light and make the sample darker, is corrected. This method has been wildly used in present studies applied in the thermal–optical transmittance (TOT) Sunset carbon analyzer based on NIOSH protocol or thermal–optical reflectance (TOR) Desert Research Institute (DRI) carbon analyzer based on IMPROVE_A protocol (Ji et al., 2016). However, the thermo-optical approach assumed that EC is the only light-absorbing species, the presence of BrC, which is part of OC but also a light-absorbing component, shifts this separation towards EC, resulting in overestimated EC values and underestimated OC values (Chen et al., 2015; Birch and Cary, 1996).

Wang et al. (2011) used a two-wavelength Aethalometer (370 and 880 nm) to identify the presence of residential wood combustion (RWC) particles which was closely associated with BrC. Organic components of wood smoke particles absorb light at 370 nm more effectively than 880 nm in two-wavelength aethalometer measurements. They believed that the enhanced absorption

https://doi.org/10.5194/amt-2020-341
Preprint. Discussion started: 9 November 2020


Atmospheric Measurement Techniques Discussions

(Delta-C=BC_{370nm}-BC_{880nm}) can serve as an indicator of RWC particles. This method was further used by Wang et al. (Wang et al., 2012a; Wang et al., 2012b). Chen et al. (2015) used a modified seven-wavelength TOT/TOR instrument (Thermal Spectral Analysis – TSA) allowing the determination of the OC-EC split at different wavelengths and light absorption measurements to be made with wavelength-specific loading corrections, providing additional information including the optical properties of black carbon (BC) and BrC from the IR to UV parts of the solar spectrum and their contributions. Massabò et al. (2016) further corrected the OC/EC split point using the Multi-Wavelength Absorbance Analyzer (MWAA) which provides the aerosol absorbance values at five wavelengths from IR to UV together with a Sunset OC/EC analyzer to achieve the BrC concentration. With a set of samples collected wintertime in the Italian Apennines, clear correlations were found between the BrC and levoglucosan mass concentration. A further step of BrC quantification taking use of TSA was reported by Chow et al. (2018), further proving that the use of seven wavelengths in thermal–optical carbon analysis allows contributions from biomass burning and secondary organic aerosols to be estimated. Their results clearly demonstrated the role of BrC in the thermo-optical analysis. However, these techniques focus on the light absorption measurement of BrC and are still limited reported in previous researches, though they provide quartz-fiber filter samples that are currently being characterized for organic carbon (OC) and EC by thermal/optical analysis. These methods mentioned above still can't achieve the observation of long-term real-time BrC mass concentrations.

Since the establishment of the thermal–optical transmittance (TOT) method by the Sunset Laboratory, the Sunset OC/EC instrument, as part of the Chemical Speciation Network (CSN), where cover over 100 monitors across the United States over 15 years, offering long-term measurement of OC and EC concentrations, has been widely used in the United States and throughout the world providing important situ data of OC and EC aerosols (U.S.EPA, 2019; Birch and Cary, 1996). This instrument had been designed with a tuned diode laser (red 660 nm) to correct the formation of pyrolyzed carbon. In this study, we modified our instrument to a two-wavelength (658 nm and 405 nm) Sunset carbon analyzer by adding one more violet diode laser at λ=405 nm. The violet diode laser together with the red diode laser, focus through the sample chamber then the laser beam passes through the filter to correct for the pyrolysis-induced error. BrC particles absorb light at 405 nm more effectively than 658 nm in two-wavelength Sunset carbon measurements. We define dEC=$EC_{405\ nm}$-$EC_{658\ nm}$ and hope it can be an indicator of BrC

https://doi.org/10.5194/amt-2020-341
Preprint. Discussion started: 9 November 2020


Atmospheric Measurement Techniques Discussions

aerosols so that we can divide real-time BrC mass concentration measurement from the two-wavelength measurement.

Nanjing, as one of the largest cities in the Yangzi River Delta region, represents a heavy industry area with a dense population. In addition, due to its topography, Nanjing is very sensitive to regional transport of air masses from its surrounding areas. OC, EC and dEC aerosols were observed from June 2015 to July 2016 at Nanjing University of Information Science and Technology (NUIST). Based on the abundant data, together with MODIS fire information, we can analyze the temporal variation, transport processes and sources of carbonaceous aerosols in North Nanjing and evaluate the biomass burning impact on dEC aerosols, which can be the scientific basis of pollution control policy.

2. Methods

2.1 Sampling

2.1.1 Study site

In this study, the sampling site is located at Nanjing University of Information Science and Technology (NUIST) in the North Suburb of Nanjing (32°207′N, 118°717′E). The study site is surrounded by housing and industrial areas. Many chemical enterprises, for example, Yangzi Petrochemical, Nanjing Chemical Industry and Nanjing Iron and Steel Group are located at the northeast of the study region, which produces exhaust with large amounts of aerosol particles. The study site is adjacent to a heavily trafficked road (Ningliu Road) located near the site, approximately 600 m to the east. Therefore, this region has intense human activities, industrial emissions and heavy traffic flow.

2.1.2 Real-time $PM_{2.5}$ observation

The real-time $PM_{2.5}$ concentrations were measured through the Tapered Element Oscillating Microbalance (TEOM) method (TEOM1405-DF, Thermo Scientific, America) during October-November in 2015, March-May, July in 2016 and January-April in 2017. The resolution of the measured data was 6 min. The instrumental operation maintenance, data assurance and quality control were performed according to the Chinese Ministry of Environmental Protection Standards for PM_{10} and $PM_{2.5}$ which was named “HJ 653-2013” (Zhang and Cao, 2015b).

2.1.3 Sample collections

$PM_{2.5}$ in the atmosphere were collected on prebaked quartz fiber filters (QFF, PALL, America) with 8*10 inch by a high volume air sampler (KC-1000, Qingdao, China) at a flow rate of 999 L

https://doi.org/10.5194/amt-2020-341
Preprint. Discussion started: 9 November 2020


Atmospheric Measurement Techniques Discussions

155 min^{-1} in four months: 4 June to 18 June, 6 October to 2 November and 10 December to 31
156 December in 2015, 10 May to 31 May in 2016. Sampling started and ended at around 8:00 and
157 20:00 every day; each sample was collected for 12 hours. A total of 148 samples were collected
158 including four field bank filters in four seasons collected following 10 mins exposures to ambient
159 air without active sampling.
160 All QFFs were pre-baked at 450 °C for 6 h before sampling to remove residual carbon. Before
161 and after sampling, all QFFs were weighed by electronic balance (Sartorius, 0.1 mg, Germany).
162 After weighting, the filters were wrapped in aluminum foils, packed in air-tight polyethylene bags
163 and stored at -20˚C for further analysis. All procedures during handling of filters were strictly
164 quality controlled to avoid any possible contamination.
165 **2.2 Two-wavelength TOT measurement**
166 Hourly concentrations of OC and EC in $PM_{2.5}$ were sampled and measured by a semi-
167 continuous carbon analyzer (Model-4, Sunset Lab, USA). Air samples were collected continuously
168 with a sample flow of ~8 L/min through a $PM_{2.5}$ cyclone. The collection time was set at 45 min
169 for each cycle. The airstream passed through a parallel plate organic denuder to reduce the effect
170 of volatile organic compounds and finally deposited on a quartz filter with a diameter of ~17mm.
171 After a sample was collected, OC and EC were analyzed using the thermal-optical
172 transmittance (TOT) method and applied a modified NIOSH 5040 protocol. Figure 1 shows the
173 structure and operational principle of the instrument. Briefly, it consists of two-stages. The oven
174 was first purged with helium and the oven temperature increased in a stepped ramp to 840℃, OC
175 was volatilized in this stage. Then the oven temperature kept at 840℃ for a while and went down
176 to 550℃. In the second stage, EC was volatilized in a second temperature ramp to 850℃ while
177 purging the oven with a mixture containing 2%oxygen and 98%helium. The pyrolysis products
178 were converted to carbon dioxide (CO_2) which was quantified using a self-contained nondispersive
179 infrared (NDIR) system.
180 Also, in this study, we used two-diode lasers (658nm and 405nm) equipped Sunset analyzer,
181 thus mass concentrations of OC and EC at different wavelengths can be measured with the 2-lasers
182 system. BrC aerosols absorb light at 405nm more significantly than 658nm in the 2-lasers system.
183 Due to the strong absorption of BrC in near-ultraviolet wavelength, thus this enhanced absorption
184 at 405nm can serve as an indicator of BrC aerosols (Liu et al., 2015). We define dEC data as the
185 difference of EC concentrations at two wavelengths ($dEC=EC_{405nm}-EC_{658nm}$) to identify the

https://doi.org/10.5194/amt-2020-341
Preprint. Discussion started: 9 November 2020


Atmospheric Measurement Techniques Discussions

presence of BrC aerosols. Our study provided a one-year measurement of dEC mass concentrations. Besides, OC and EC represent the OC and EC concentrations at 658nm in this paper without a special explanation.

At the end of each analysis, a fixed volume of an internal standard containing 5%methane and 95%Helium was injected and thus a known carbon mass could be derived. The external sucrose standard (4.207 μg μL^{-1}) calibration was conducted every week to insure repeatable quantification. Calibration with an instrument blank was conducted every day. Both detection limit for OC and EC of the instrument was 0.5 μg m^{-3}. We also did the measurements of OC and EC in $PM_{2.5}$ filter samples using the same method followed by the NIOSH protocol. Figure S1 shows the correlations between the real-time OC, EC concentrations and sampling OC, EC concentrations at the same time. The results showed that the online and offline data during the corresponding periods had good correlations with $R^2$of 0.81 for OC, $R^2$of 0.41 for EC and R^2 of 0.82 for TC.

2.3 Identification of potential regional sources

The Hybrid Single-Particle Lagrangian Integrated Trajectory (HYSLPIT4.8) model, provided by the National Oceanic and Atmospheric Administration (NOAA) were used to investigate the air mass origins of carbonaceous aerosols. The 48-hour back trajectories at Nanjing (32.2°N, 118.7°E) were calculated every hour (Draxler and Hess, 1998). In order to evaluate the behavior of the air masses circulation in the planetary boundary layer (PBL), the trajectories at 500m corresponding to the upper-middle height of the PBL were calculated, representing well-mixed convective boundary layer for regional transport investigation (Xu and Akhtar, 2010). The National Center for Environmental Prediction Global Data Assimilation System (NCEP GDAS) data obtained from NOAA with a spatial resolution of 1° ×1° and 24 levels of the vertical resolution were used as meteorological data input to the model. The Potential Source Contribution Function (PSCF) model was usually applied to localize the potential sources of pollutants. The details about the setup of the model can be seen in the research reported by Bao et al. (2017).

3. Results and discussion

3.1 Characteristics of carbonaceous aerosols

3.1.1 Concentrations of carbonaceous aerosols

The statistics for the $PM_{2.5}$, OC, EC and dEC mass concentrations at the NUIST site are summarized in Table 1. The hourly OC concentrations ranged from 0.5 to 45.8 μg m^{-3} (average of 8.9 ± 5.5 μg m^{-3}), and the EC concentrations ranged from 0.0 to 17.6 μg m^{-3} (average of 3.1 ± 2.0

https://doi.org/10.5194/amt-2020-341
Preprint. Discussion started: 9 November 2020


Atmospheric Measurement Techniques Discussions

μg m^{-3}). The results were comparable to those reported by Chen et al. (2017) in the Xianlin Campus of Nanjing University (5.7 μg m^{-3} for OC and 3.2 μg m^{-3} for EC), which site was located in the southeast suburb of Nanjing and close to the G25 highway and were also affected by traffic sources. The higher OC concentrations in this study were probably due to the around chemical enterprise emissions. The average contributions of OC and EC to the total measured $PM_{2.5}$ mass was 12.8% and 4.3%, respectively, suggesting that carbonaceous fraction made an important contribution to fine particulate matter. The average dEC mass concentration was 0.8 μg m^{-3} contributing 10.0% to OC and 1.3% to $PM_{2.5}$ concentrations with max concentration of 8.1 μg m^{-3} contributing 48.2% to OC and 17.6% to total $PM_{2.5}$ concentrations.

Compared with carbonaceous aerosols levels in other cities (Table S1), the OC and EC concentrations in Nanjing were generally lower than those observed in megacities such as Beijing and Shanghai and inland cities like Chengdu and Chongqing which was affected by the basin terrain characteristics with static wind and unfavorable diffusion conditions, but higher than those observed in the southern coastal cities such as Guangzhou and Hongkong. In general, the level of carbonaceous aerosols concentrations in China was higher than that in developed countries in the United States and Europe and lower than that in developing countries like India. The average OC/EC ratios in this study was 3.6, which was lower than most of those reported in other studies, indicating the important impact of vehicle emissions in our study site.

Figure 2 shows the mass fractions of hourly carbonaceous aerosols and OC/EC ratios at different $PM_{2.5}$ concentration intervals during the study periods. During the study period, 84.2% of the $PM_{2.5}$ samples exceeded the daily averaged Chinese national ambient air quality standard (NAAQS) of 35.0 μg m^{-3} for the first grade and 40.1% of the total samples exceeded the NAAQS of 75.0 μg m^{-3} for the second grade, reflecting heavy aerosol pollution in the study area. Generally, the fractions of carbonaceous components decreased with increasing $PM_{2.5}$ pollution level. Larger mass fraction (about 32.3%) of carbonaceous aerosols in $PM_{2.5}$ was found for period relatively lower $PM_{2.5}$ levels (0–20 μg m^{-3}) compared to high $PM_{2.5}$ levels (300–500 μg m^{-3}) with carbonaceous aerosols mass fraction of 5.2%. The result indicated other components like secondary inorganic aerosol (SIA) contributes more significantly to heavy haze events in Nanjing, which was also found in other cities in the Yangtze River Delta area (Yang et al., 2011; Zhang and Zhang, 2019). The contribution of dEC to OC decreased with the increase of $PM_{2.5}$ concentrations between 0-200 μg m^{-3}, and then increased with the increase of $PM_{2.5}$ concentrations between 200-

https://doi.org/10.5194/amt-2020-341
Preprint. Discussion started: 9 November 2020


Atmospheric Measurement Techniques Discussions

500 μg m^{-3}. The dEC contributed most significantly to OC of 14.3% when $PM_{2.5}$ concentrations below 20 μg m^{-3}. Similar trend was found in OC/EC ratios which showed a sharp increase along with enhanced $PM_{2.5}$ level above 150 μg m^{-3}. Previous studies had reported that high OC/EC ratios were related to SOC formation or biomass burning emissions whereas low OC/EC ratios were related to vehicle exhaust (Wang et al., 2015). We devided the dEC/OC at different intervals of OC/EC ratios and found that the dEC/OC increased when the OC/EC ratios increased in four seasons, indicating strong secondary sources or biomass burning contributions to dEC during heavy pollution periods (Fig. S2).

3.1.2 Seasonal variations of carbonaceous aerosols

As shown in Fig. 3, the OC, EC concentrations and dEC/OC ratios showed similar variations with highest in winter and lowest in summer. The average OC concentration in winter was ~1.4 times higher than that in summer and the average EC concentrations and dEC/OC in winter were approximately 1.5 and 1.6 times higher than those in summer. The seasonality of carbonaceous species in $PM_{2.5}$ was strongly influenced by seasonal variations in emissions intensities and meteorological parameters. Table S2 summarizes the meteorological parameters in four seasons during the study period. The high carbonaceous aerosols concentrations in winter were mainly a result of relatively stable atmospheric conditions with low temperature, relative humidity and boundary layer on one hand, and on the other hand, increasing emissions from fossil-fuel combustion for heating from the chemical enterprises nearby. In summer, higher boundary layer resulted in the dispersion of aerosols in the atmosphere, and higher temperature promoted the partitioning of semi-volatile organic compounds (SVOCs) into gaseous phase (Yang et al., 2011). In addition, large precipitation in summer (586 mm in total) favored the wet scavenging processes of aerosols.

The OC/EC ratios in spring, summer, autumn and winter were 3.9, 4.0, 2.8 and 3.4, respectively. The OC/EC ratio could give some information about primary and secondary organic carbon (Turpin and Huntzicker, 1995; Lim and Turpin, 2002). In summer, strong convective activities in the atmospheric boundary layer and solar radiation, high temperature and plenty of moisture in the atmosphere were favorable for the formation of SOC. On the other hand, the high OC/EC ratios in June in this study were also strongly related to biomass burning which will be discussed in the 3.3 sections. The lower ratios of OC to EC in autumn and winter indicated that strong primary sources in these two seasons.

https://doi.org/10.5194/amt-2020-341
Preprint. Discussion started: 9 November 2020


Atmospheric Measurement Techniques Discussions

279 3.1.3 Diurnal variation of carbonaceous aerosols

280 The diurnal pattern of carbonaceous aerosols can be affected by both mereorological
281 parameters and sources (Ji et al., 2016). Figure 4 depicts the diurnal variation of OC, EC, dEC/OC
282 and OC/EC ratios during the study period. Clear diurnal variations were observed in OC and EC
283 aerosols. Both the OC and EC concentrations kept high levels at night and low levels in the daytime,
284 indicating the strong influence of the atmospheric boundary layer on air quality in the northern
285 Nanjing. The peak occurred in the morning both in OC and EC indicating the significant impact
286 of traffic source on the OC and EC concentrations. The dEC/OC and OC/EC ratios showed similar
287 trends in the daytime with gradually increase from morning till afternoon, indicating the
288 importance of the contribution of secondary sources to dEC. It should be noted that the vehicle
289 emissions and the boundary layer height had no significant effect on the diurnal variation of
290 dEC/OC, suggesting there was no significant local sources of dEC. There was a small peak in
291 dEC/OC at 3:00 am, which might be related to the aqueous secondary organic aerosols formations
292 during nighttime (Sullivan et al., 2016).

293 The relative humidity (RH) and Temperature (T) dependent distributions of OC, EC mass
294 concentrations and dEC/OC and OC/EC throughout the study period are shown in Fig. 5. We also
295 found similar distributions in dEC/OC and OC/EC. High dEC/OC (>30 %) could be found in three
296 areas, first showed in the right area with relatively high T at 25-40 ℃ and RH at 40-60 %, which
297 were usually found in the summer afternoon which was closely related to the strong formation of
298 SOC. The second area was displayed in the upper region with RH over 80 % and T at 10-20 ℃
299 and the third area appeared when RH below 30 % and T at about 10 ℃, corresponding to nighttime
300 and winter afternoon. The OC and EC showed similar distributions with the highest mass loading
301 (OC: > 20 μg m^{-3}; EC: > 8 μg m^{-3}) at relatively high RH at 60-80 % which usually occurred at
302 night with relatively low boundary layer height, leading to the accumulation of aerosols.

303 **3.2 Air aass transport**

304 3.2.1 Windrose of carbonaceous aerosols

305 To investigate the influences of air masses transport to the study site, the wind rose of OC, EC
306 and dEC/OC using hourly data in four seasons is illustrated in Fig. 6. Two points should be noted.
307 First, high OC and EC mass concentrations were found near the field site (indicating by WS < 1
308 m s^{-1}), suggesting that local and primary emissions (e.g., industrial and vehicle emissions) were
309 stable and important sources contributing to atmospheric OC and EC mass concentrations in

https://doi.org/10.5194/amt-2020-341
Preprint. Discussion started: 9 November 2020


Atmospheric Measurement Techniques Discussions

northern Nanjing. The OC mass concentrations from the southwest increased with the increase of WS in summer, indicating that sources of OC are complicated in summer including secondary reaction during long-range or regional transport. Second, compared with OC and EC, dEC aerosols showed no significant local sources. The dEC/OC increased with the increasing of WS and highest dEC/OC were found when WS over 3 m s^{-1}. Long-range or regional transport was highly likely the main sources contributing to dEC mass concentrations.

3.2.2 The potential source areas of carbonaceous aerosols

The possible source contributions were evaluated using the PSCF model and the PSCF map are shown in Fig. 7. The areas with high PSCF values were highly likely the potential pollution source areas. As shown in Fig. 7, PSCF results further proved the strong regional transport contribution to dEC aerosols and local contributions to OC and EC aerosols. In spring, the potential source areas of OC and EC were mainly from the southwest of Nanjing, however, the potential source areas of dEC aerosols were from the east of Nanjing, indicating obvious different sources between OC, EC and dEC. In summer, Local areas were the main sources areas of EC and the near-by Yangtze River Delta City Group from southeast of Nanjing including developed cities like Shanghai were the main sources areas of OC and dEC. The anthropogenic emissions from these areas might be important sources of OC and dEC. Besides, both the potential sources areas of dEC and EC were displayed in the northwest of Nanjing in summer, suggesting strong primary sources of dEC from this area which were very likely associated to biomass burning, more details were in the section 3.3. In autumn, strongest local sources from the study site of OC and EC were found. However the dEC mainly originated from regional transport from the northwest and southeast areas of Nanjing. Biomass burning has been proved to be an important source of air pollutants in the Yangtze River Delta (YRD) area, especially in the wheat harvest seasons (e.g., June and October) (Cheng et al., 2014; Zhang and Cao, 2015a). In addition, the YRD area is the most economically developed region in China and has lots of industrial cities, which means that industrial emissions and anthropogenic sources contributed to high carbonaceous aerosols pollution levels. In winter, dEC were mainly from long-range transport from northern cities and regional transport from the southwest areas of Nanjing while both long-range transport and local sources were found in OC and EC concentrations.

3.3 The characteristics of carbonaceous aerosols during biomass burning periods

The biomass burning emission has been proved to be an important source of BrC on a globle

https://doi.org/10.5194/amt-2020-341
Preprint. Discussion started: 9 November 2020


Atmospheric Measurement Techniques Discussions

scale, it is consistently observed in large-scale forest fire events (Laskin et al., 2015). Based on the Fire Information for Resource Management System (FIRMS) derived from the Moderate Resolution Imaging Spectroradiometer (MODIS), we found that the fire points reached to 2028, 1773 and 967 on 11 Jun 2015, 7 February 2016 and 2 Mar 2016 in the areas around our study site, respectively, suggesting there were strong biomass burning events on these days (Fig. S3). To further investigate the biomass burning impact on dEC aerosols, we analyzed the temporal trends of carbonaceous aerosols from 4 June 2015 to 19 June 2015 and 7 February 2016 to 3 Mar 2016, respectively. Combining the observed aerosols concentrations and fire information, we divided the periods into normal days and biomass burning days. It should be noted that the biomass burning days are not determined based only on fire points. We also considered the 48-h backward trajectories and open biomass burning areas. For example, we did found lots of fire points from 11 June 2015 to 12 June 2015 and from 7 February 2016 to 10 February 2016, respectively, and the 48-h back trajectories went through these biomass burning areas (Fig. S4b, c). However, although there were large amounts of fire points in northwest of Nanjing from 8 June 2015 to 9 June 2015, the backward trajectory showed air mass during the periods came from the southeast areas where no open fire points were found (Fig. S4a). In contrast, there were only a few fire points found near the study site from 26 February 2016 to 27 February 2016, the 48-h backward trajectory showed the air mass was exactly from the area (Fig. S4d).

As shown in Fig. 8 and Fig. 9, we found that dEC concentrations, dEC/OC and OC/EC ratios showed peaks during each biomass burning periods which was not that obvious in OC and EC concentrations, suggesting the unique biomass burning impact on dEC and the sources of OC and EC were more complicated. It should be noted that there were peaks of dEC appeared on 9 June 2015 and 13 February 2016, which were not biomass burning days, suggesting that biomass burning was not the only sources of dEC. As mentioned in the 3.1 and 3.2 section, anthropogenic emissions could be the sources of dEC and the secondary sources couldn't be ignored, too. Summarized in Table 2 are the average and standard deviation values of OC, EC, OC/EC, dEC and dEC/OC during biomass burning and normal days. The OC/EC, dEC concentrations and dEC/OC were obvious higher in biomass burning days than those in normal days, but similar levels of the OC and EC concentrations were found both in biomass burning days and normal days in summer, suggesting the great contribution of biomass burning emissions to dEC aerosols and there were other sources of OC and EC in summer. All the carbonaceous aerosols were higher in biomass

https://doi.org/10.5194/amt-2020-341
Preprint. Discussion started: 9 November 2020


Atmospheric Measurement Techniques Discussions

372 burning days in winter, in addition, the location of open fire counts were mainly in the northwest
373 and southwest area of the study site (Fig. S4c, d), which were the potential source areas of OC, EC
374 and dEC in winter as discussed in the section 3.2.2, indicating strong contributions of biomass
375 burning emissions to all the carbonaceous aerosols in winter.

376 **4. Conclusion**

377 In this study, the characteristics and sources of carbonaceous aerosols in North Nanjing were
378 investigated and we introduced a two-wavelength method by modifying the Sunset carbon analyzer.
379 We incorpated a new diode laser at λ=405 nm in the instrument, making it possible to detect the
380 laser beam passing through the filter at both wavelength at λ=658 nm and λ=405 nm, so we can
381 obtain the dEC concentrations. Our study illustrated the feasibility of using dEC to characterize
382 the BrC aerosols, providing a new idea about the measurement of BrC. The results showed that
383 high (low) OC, EC and dEC concentrations were found in Winter (summer), indicating the
384 significant impact of the increase of various emission sources in winter and wet scavenging of rain
385 in summer. Similar diurnal cycles for OC and EC concentrations were found with high at night
386 and low in daytime, strongly affected by the boundary layers. Traffic emissions were found to have
387 significant influence on the concentrations of OC and EC. Similar trends were found in the diurnal
388 cycle of dEC/OC and OC/EC and the dEC/OC increased when the OC/EC ratios increased,
389 indicating strong secondary sources or biomass burning impact on dEC. The wind rose and
390 receptor model results showed that strong local emissions were found in OC and EC aerosols,
391 however dEC aerosols were significantly affected by regional or long-range transport. The near-
392 by YRD area was one of the main potential source areas of dEC, suggesting that anthropogenic
393 emissions could be the sources of dEC. Together with the back trajectories analysis and MODIS
394 fire informations, we analyzed two biomass burning events both in summer and winter. The results
395 showed that the sources of OC and EC were more complicated than those of dEC aerosols in
396 summer. Biomass burning emission made a great contribution to dEC concentrations in summer.
397 Large number of open fire counts from the northwest and southwest areas of the study site were
398 monitored, significantly contributed to all the carbonaceous aerosols pollutions in winter.

399 Our modified two-wavelength instrument provided more information than traditional single-
400 wavelength thermo/optical carbon analyzer. The results proved that dEC can be an indicator of
401 BrC in biomass burning days. It should be noted that the sources of dEC were complicated and the
402 anthropogenic emissions and secondary formations of dEC aerosols couldn't be ignored , further

https://doi.org/10.5194/amt-2020-341
Preprint. Discussion started: 9 November 2020


Atmospheric Measurement Techniques Discussions

chemical analysis need to be conducted in the future. We also hope that the dEC data can be further applied in more researches.

Acknowledgments

This research is financially supported by the National Natural Science Foundation of China (grant no. 41977305), the Provincial Natural Science Foundation of Jiangsu (grant no. BK20180040) and the Postgraduate Research & Practice Innovation Program of Jiangsu Province (grant no. KYCX18_1014). This study is supported by the funding of Jiangsu Innovation & Entrepreneurship Team. The authors would also like to thank the China Scholarship Council for the support to Mengying Bao.We would also like to express our gratitude to Yuanyuan Zhang, Zufei Xu and Tianran Zhang for their assistance in the instrument maintenance throughout the obsevation period. Besides, we are grateful for Prof. Yunhua Chang, who makes considerable comments and suggerestions to this paper.

References:

Andreae, M. O. and Gelencsér, A.: Black carbon or brown carbon? The nature of light-absorbing carbonaceous aerosols, Atmos. Chem. Phys., 6, 3131–3148, 2006.

Arola, A., Schuster, G., Myhre, G., Kazadzis, S., Dey, S., and Tripathi, S. N.: Inferring absorbing organic carbon content from AERONET data, Atmos. Chem. Phys., 11, 215-225, 10.5194/acp-11-215-2011, 2011.

Bao, M., Cao, F., Chang, Y., Zhang, Y.-L., Gao, Y., Liu, X., Zhang, Y., Zhang, W., Tang, T., Xu, Z., Liu, S., Lee, X., Li, J., and Zhang, G.: Characteristics and origins of air pollutants and carbonaceous aerosols during wintertime haze episodes at a rural site in the Yangtze River Delta, China, Atmos. Pollut. Res., 8, 900-911, 10.1016/j.apr.2017.03.001, 2017.

Birch, M. E. and Cary, R. A.: Elemental carbon-based method for occupational monitoring of particulate diesel exhaust: methodology and exposure issues, Analyst, 121, 1183-1190, 1996.

Cao, F. and Zhang, Y.-L.: Principle，method development and application of radiocarbon (^{14}C) —based source apportionment of carbonaceous aerosols: a review, Adv. Earth Sci., 30, 425-432, 10.11867 / j. issn. 1001-8166. 2015. 04. 0425., 2015.

Chen, L. W. A., Chow, J. C., Wang, X. L., Robles, J. A., Sumlin, B. J., Lowenthal, D. H., Zimmermann, R., and Watson, J. G.: Multi-wavelength optical measurement to enhance

https://doi.org/10.5194/amt-2020-341
Preprint. Discussion started: 9 November 2020


Atmospheric Measurement Techniques Discussions

thermal/optical analysis for carbonaceous aerosol, Atmos. Meas. Tech., 8, 451-461, 10.5194/amt-8-451-2015, 2015.

Cheng, Z., Wang, S., Fu, X., Watson, J. G., Jiang, J., Fu, Q., Chen, C., Xu, B., Yu, J., Chow, J. C., and Hao, J.: Impact of biomass burning on haze pollution in the Yangtze River delta, China: a case study in summer 2011, Atmos. Chem. Phys., 14, 4573-4585, 10.5194/acp-14-4573-2014, 2014.

Chow, J. C., Watson, J. G., Chen, L.-W. A., Arnott, W. P., Moosmüller, H., and Fung, K.: Equivalence of elemental carbon by thermal/optical reflectance and transmittance with different temperature protocols, Envirn. Sci. Technol., 38, 4414-4422, 10.1021/es034936u 2004.

Draxler, R. R., and Hess, G. D.: An overview of the HYSPLIT_4 modelling system for trajectories, dispersion, and deposition, Aust. Meteorol. Mag., 47, 295-308, 1998.

Feng, Y., Ramanathan, V., and Kotamarthi, V. R.: Brown carbon: a significant atmospheric absorber of solar radiation?, Atmos. Chem. Phys., 13, 8607-8621, 10.5194/acp-13-8607-2013, 2013.

Huang, R. J., Zhang, Y., Bozzetti, C., Ho, K. F., Cao, J. J., Han, Y., Daellenbach, K. R., Slowik, J. G., Platt, S. M., Canonaco, F., Zotter, P., Wolf, R., Pieber, S. M., Bruns, E. A., Crippa, M., Ciarelli, G., Piazzalunga, A., Schwikowski, M., Abbaszade, G., Schnelle-Kreis, J., Zimmermann, R., An, Z., Szidat, S., Baltensperger, U., El Haddad, I., and Prevot, A. S.: High secondary aerosol contribution to particulate pollution during haze events in China, Nature, 514, 218-222, 10.1038/nature13774, 2014.

Ji, D., Zhang, J., He, J., Wang, X., BoPanga, Liua, Z., Wang, L., and Wang, Y.: Characteristics of atmospheric organic and elemental carbon aerosols in urban Beijing, China, Atmos. Environ., 293-306, 10.1016/j.atmosenv.2015.11.020, 2016.

Kirillova, E. N., Andersson, A., Han, J., Lee, M., and Gustafsson, O.: Sources and light absorption of water-soluble organic carbon aerosols in the outflow from northern China, Atmos. Chem. Phys., 14, 1413-1422, 10.5194/acp-14-1413-2014, 2014.

Laskin, A., Laskin, J., and Nizkorodov, S. A.: Chemistry of atmospheric brown carbon, Chemical Reviews, 115, 4335-4382, 10.1021/cr5006167, 2015.

Lei, Y., Shen, Z., Zhang, T., Zhang, Q., Wang, Q., Sun, J., Gong, X., Cao, J., Xu, H., Liu, S., and Yang, L.: Optical source profiles of brown carbon in size-resolved particulate matter from typical domestic biofuel burning over Guanzhong Plain, China, Sci. Total. Environ., 622-623, 244-251, 10.1016/j.scitotenv.2017.11.353, 2018.

https://doi.org/10.5194/amt-2020-341
Preprint. Discussion started: 9 November 2020


Atmospheric Measurement Techniques Discussions

Lelieveld, J., Evans, J. S., Fnais, M., Giannadaki, D., and Pozzer, A.: The contribution of outdoor air pollution sources to premature mortality on a global scale, Nature, 525, 367-371, 10.1038/nature15371, 2015.

Li, C., He, Q., Hettiyadura, A. P. S., Kafer, U., Shmul, G., Meidan, D., Zimmermann, R., Brown, S. S., George, C., Laskin, A., and Rudich, Y.: Formation of secondary brown carbon in biomass burning aerosol proxies through NO_3 radical reactions, Environ. Sci. Technol., 54, 1395-1405, 10.1021/acs.est.9b05641, 2020.

Lim, H.-J. and Turpin, B. J.: Origins of primary and secondary organic aerosol in Atlanta: results of time-resolved measurements during the Atlanta supersite experiment, Environ. Sci. Technol., 36, 4489-4496, 10.1021/es0206487 2002.

Liu, S., Aiken, A. C., Gorkowski, K., Dubey, M. K., Cappa, C. D., Williams, L. R., Herndon, S. C., Massoli, P., Fortner, E. C., Chhabra, P. S., Brooks, W. A., Onasch, T. B., Jayne, J. T., Worsnop, D. R., China, S., Sharma, N., Mazzoleni, C., Xu, L., Ng, N. L., Liu, D., Allan, J. D., Lee, J. D., Fleming, Z. L., Mohr, C., Zotter, P., Szidat, S., and Prevot, A. S. H.: Enhanced light absorption by mixed source black and brown carbon particles in UK winter, Nat. Commun., 6, 8435, 10.1038/ncomms9435, 2015.

Liu, X., Zhang, Y.-L., Peng, Y., Xu, L., Zhu, C., Cao, F., Zhai, X., Haque, M. M., Yang, C., Chang, Y., Huang, T., Xu, Z., Bao, M., Zhang, W., Fan, M., and Lee, X.: Chemical and optical properties of carbonaceous aerosols in Nanjing, eastern China: regionally transported biomass burning contribution, Atmos. Chem. Phys., 19, 11213-11233, 10.5194/acp-19-11213-2019, 2019.

Saleh, R., Robinson, E. S., Tkacik, D. S., Ahern, A. T., Liu, S., Aiken, A. C., Sullivan, R. C., Presto, A. A., Dubey, M. K., Yokelson, R. J., Donahue, N. M., and Robinson, A. L.: Brownness of organics in aerosols from biomass burning linked to their black carbon content, Nat. Geosci., 7, 647-650, 10.1038/ngeo2220, 2014.

Satish, R., Shamjad, P., Thamban, N., Tripathi, S., and Rastogi, N.: Temporal characteristics of brown carbon over the central Indo-Gangetic Plain, Environ. Sci. Technol., 51, 6765-6772, 10.1021/acs.est.7b00734, 2017.

Sullivan, A. P., Hodas, N., Turpin, B. J., Skog, K., Keutsch, F. N., Gilardoni, S., Paglione, M., Rinaldi, M., Decesari, S., Facchini, M. C., Poulain, L., Herrmann, H., Wiedensohler, A., Nemitz, E., Twigg, M. M., and Collett Jr, J. L.: Evidence for ambient dark aqueous SOA formation in the Po Valley, Italy, Atmos. Chem. Phys., 16, 8095-8108, 10.5194/acp-16-8095-2016, 2016.

https://doi.org/10.5194/amt-2020-341
Preprint. Discussion started: 9 November 2020


Atmospheric Measurement Techniques Discussions

496 Turpin, B. J. and Huntzicker, J.: Identification of secondary organic aerosol episodes and
497 quantitation of frimary and secondary organic aerosol concentrations during SCAQS, Atmos.
498 Environ., 29, 3527-3544, 1995.
499 U.S.EPA: Review of sunset organic and elemental carbon (OC and EC) measurements during
500 EPA's sunset carbon evaluation project, prepared by Sonoma Technology, Inc., CA 94954-6515,
501 prepared for U.S. Environmental Protection Agency, NC 27711, 2019.
502 Wang, J., Nie, W., Cheng, Y., Shen, Y., Chi, X., Wang, J., Huang, X., Xie, Y., Sun, P., Xu, Z., Qi,
503 X., Su, H., and Ding, A.: Light absorption of brown carbon in eastern China based on 3-year multi-
504 wavelength aerosol optical property observations and an improved absorption Ångström exponent
505 segregation method, Atmos. Chem. Phys., 18, 9061-9074, 10.5194/acp-18-9061-2018, 2018.
506 Wang, P., Cao, J. J., Shen, Z. X., Han, Y. M., Lee, S. C., Huang, Y., Zhu, C. S., Wang, Q. Y., Xu,
507 H. M., and Huang, R. J.: Spatial and seasonal variations of $PM_{2.5}$ mass and species during 2010 in
508 Xi'an, China, Sci. Total. Environ., 508, 477-487, 10.1016/j.scitotenv.2014.11.007, 2015.
509 Wang, Y., Hopke, P. K., and Rattigan, O. V.: A new indicator of fireworks emissions in Rochester,
510 New York, Environ. Monit. Assess., 184, 7293-7297, 10.1007/s10661-011-2497-5, 2012a.
511 Wang, Y., Hopke, P. K., Rattigan, O. V., Chalupa, D. C., and Utell, M. J.: Multiple-year black
512 carbon measurements and source apportionment using delta-C in Rochester, New York, J. Air
513 Waste Manag. Assoc., 62, 880-887, 10.1080/10962247.2012.671792, 2012b.
514 Wu, C. and Yu, J. Z.: Determination of primary combustion source organic carbon-to-elemental
515 carbon (OC/EC) ratio using ambient OC and EC measurements: secondary OC-EC correlation
516 minimization method, Atmos. Chem. Phys., 16, 5453-5465, 10.5194/acp-16-5453-2016, 2016.
517 Wu, G., Wan, X., Ram, K., Li, P., Liu, B., Yin, Y., Fu, P., Loewen, M., Gao, S., Kang, S., Kawamura,
518 K., Wang, Y., and Cong, Z.: Light absorption, fluorescence properties and sources of brown carbon
519 aerosols in the Southeast Tibetan Plateau, Environ. Pollut., 257, 113616,
520 10.1016/j.envpol.2019.113616, 2020.
521 Xu, X. and Akhtar, U. S.: Identification of potential regional sources of atmospheric total gaseous
522 mercury in Windsor, Ontario, Canada using hybrid receptor modeling, Atmos. Chem. Phys., 10,
523 7073-7083, 10.5194/acp-10-7073-2010, 2010.
524 Yan, C., Zheng, M., Bosch, C., Andersson, A., Desyaterik, Y., Sullivan, A. P., Collett, J. L., Zhao,
525 B., Wang, S., He, K., and Gustafsson, O.: Important fossil source contribution to brown carbon in
526 Beijing during winter, Sci. Rep., 7, 10.1038/srep43182, 2017.

https://doi.org/10.5194/amt-2020-341
Preprint. Discussion started: 9 November 2020


Atmospheric Measurement Techniques Discussions

527 Yang, F., Tan, J., Zhao, Q., Du, Z., He, K., Ma, Y., Duan, F., Chen, G., and Zhao, Q.: Characteristics
528 of $PM_{2.5}$ speciation in representative megacities and across China, Atmos. Chem. Phys., 11, 5207-
529 5219, 10.5194/acp-11-5207-2011, 2011.
530 Zhang, Q., Shen, Z., Zhang, L., Zeng, Y., Ning, Z., Zhang, T., Lei, Y., Wang, Q., Li, G., Sun, J.,
531 Westerdahl, D., Xu, H., and Cao, J.: Investigation of primary and secondary particulate brown
532 carbon in two Chinese cities of Xi'an and Hong Kong in wintertime, Environ. Sci. Technol., 54,
533 3803-3813, 10.1021/acs.est.9b05332, 2020.
534 Zhang, W. and Zhang, Y.: Oxygen isotope anomaly ($\Delta^{17}O$) in atmospheric nitrate: a review,
535 Chinese Sci. Bull., 64, 649-662, 10.1360/n972018-01028, 2019.
536 Zhang, W., Zhang, Y.-L., Cao, F., Xiang, Y., Zhang, Y., Bao, M., Liu, X., and Lin, Y.-C.: High time-
537 resolved measurement of stable carbon isotope composition in water-soluble organic aerosols:
538 method optimization and a case study during winter haze in eastern China, Atmos. Chem. Phys.,
539 19, 11071-11087, 10.5194/acp-19-11071-2019, 2019.
540 Zhang, X., Lin, Y.-H., Surratt, J. D., Zotter, P., Prevot, A. S. H., and Weber, R. J.: Light-absorbing
541 soluble organic aerosol in Los Angeles and Atlanta: a contrast in secondary organic aerosol,
542 Geophys. Res. Lett., 38, 10.1029/2011gl049385, 2011.
543 Zhang, Y. and Kang, S.: Characteristics of carbonaceous aerosols analyzed using a
544 multiwavelength thermal/optical carbon analyzer: a case study in Lanzhou City, Sci. China Earth
545 Sci., 62, 389-402, 10.1007/s11430-017-9245-9, 2019.
546 Zhang, Y., Ren, H., Sun, Y., Cao, F., Chang, Y., Liu, S., Lee, X., Agrios, K., Kawamura, K., Liu,
547 D., Ren, L., Du, W., Wang, Z., Prevot, A. S. H., Szida, S., and Fu, P.: High contribution of nonfossil
548 sources to submicrometer organic aerosols in Beijing, China, Environ. Sci. Technol., 51, 7842-
549 7852, 10.1021/acs.est.7b01517, 2017.
550 Zhang, Y.-L. and Cao, F.: Is it time to tackle $PM_{2.5}$ air pollutions in China from biomass-burning
551 emissions?, Environ. Pollut., 202, 217-219, 10.1016/j.envpol.2015.02.005, 2015a.
552 Zhang, Y. L. and Cao, F.: Fine particulate matter ($PM_{2.5}$) in China at a city level, Sci. Rep., 5,
553 14884, 10.1038/srep14884, 2015b.
554 Zhou, S., Wang, T., Wang, Z., Li, W., Xu, Z., Wang, X., Yuan, C., Poon, C. N., Louie, P. K. K.,
555 Luk, C. W. Y., and Wang, W.: Photochemical evolution of organic aerosols observed in urban
556 plumes from Hong Kong and the Pearl River Delta of China, Atmos. Environ., 88, 219-229,
557 10.1016/j.atmosenv.2014.01.032, 2014.

https://doi.org/10.5194/amt-2020-341
Preprint. Discussion started: 9 November 2020

Atmospheric Measurement Techniques Discussions

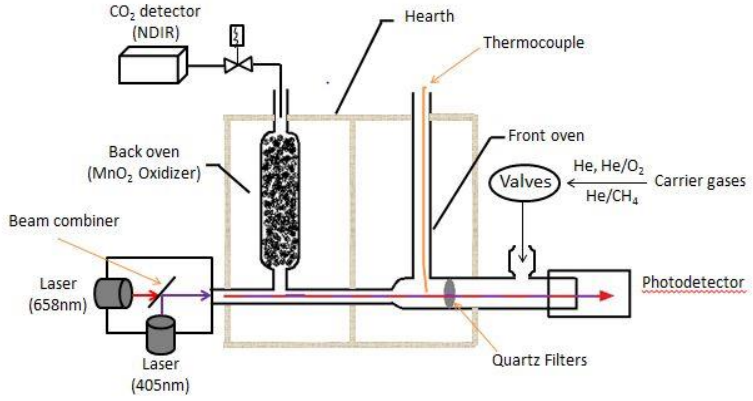

558

559 **Figure 1**. Principle and structure of the sunset semi-continuous carbon analyzer.

https://doi.org/10.5194/amt-2020-341
Preprint. Discussion started: 9 November 2020

Atmospheric Measurement Techniques Discussions

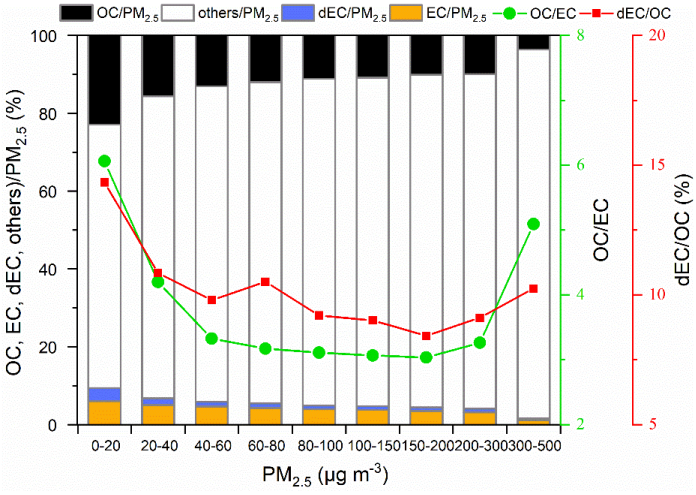

Figure 2. Carbonaceous species fractions of $PM_{2.5}$ and OC/EC ratios at different $PM_{2.5}$ concentration intervals at NUIST from June 2015 to August 2016.

https://doi.org/10.5194/amt-2020-341
Preprint. Discussion started: 9 November 2020

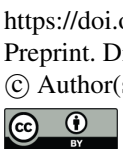

Atmospheric Measurement Techniques Discussions

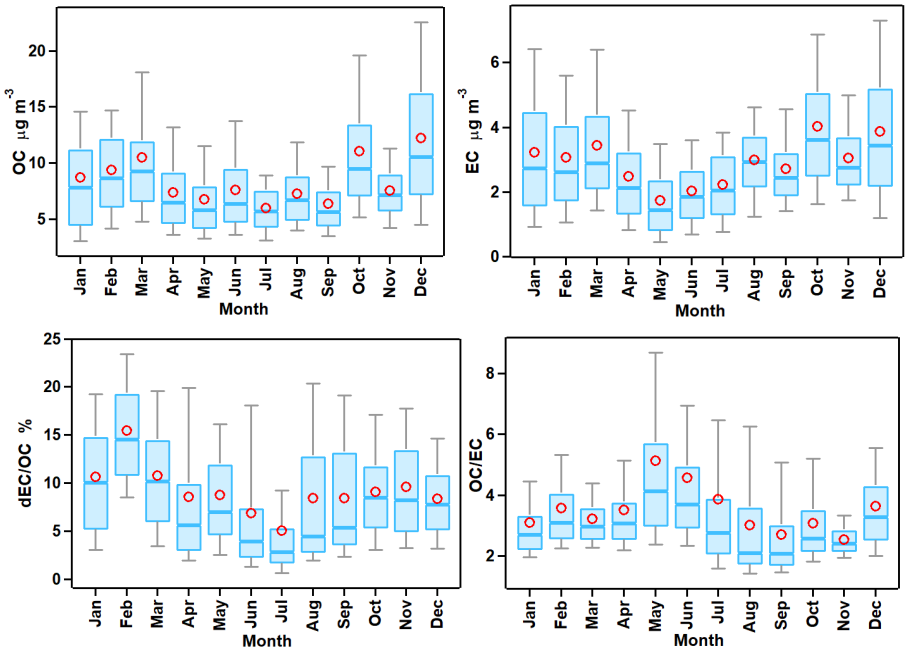

Figure 3. Monthly variations of OC, EC, dEC/OC and OC/EC ratios at NUIST from June 2015 to August 2016. The boundary of the box indicates the 25% and 75% percentile, respectively. The lower and upper whiskers indicate the 10% and 90% percentile, respectively. The red circle within the box marks the average while the line within the box marks the median.

https://doi.org/10.5194/amt-2020-341
Preprint. Discussion started: 9 November 2020

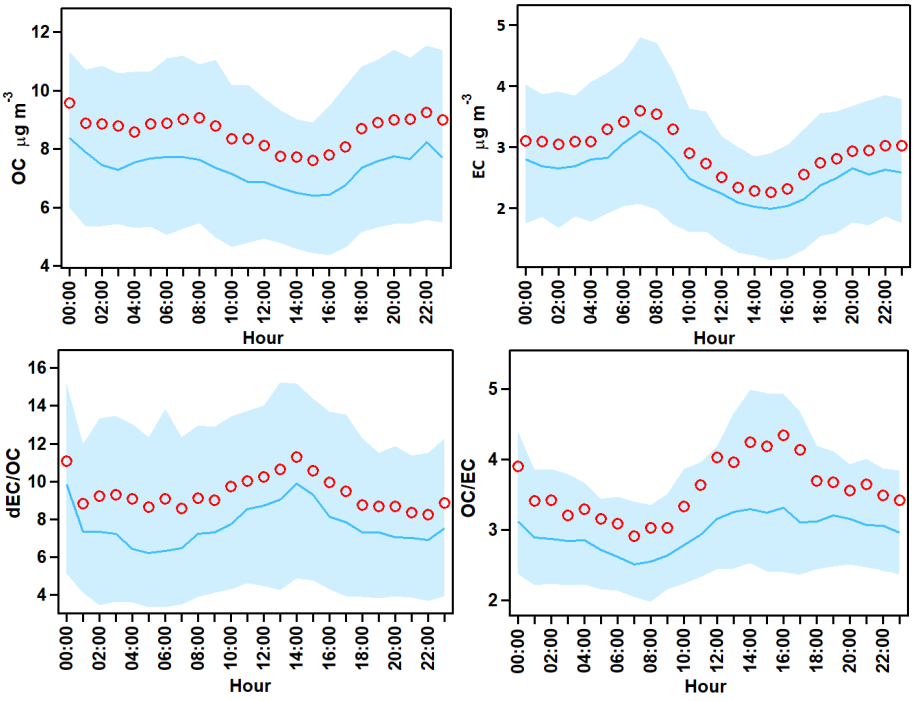

Figure 4. Diurnal variations of OC, EC concentrations, dEC/OC and OC/EC ratios during the study period. The boundary of the shaded area indicates the 25% and 75% percentile, respectively. The red circle marks the average while the blue line marks the median.

https://doi.org/10.5194/amt-2020-341
Preprint. Discussion started: 9 November 2020

Atmospheric Measurement Techniques Discussions

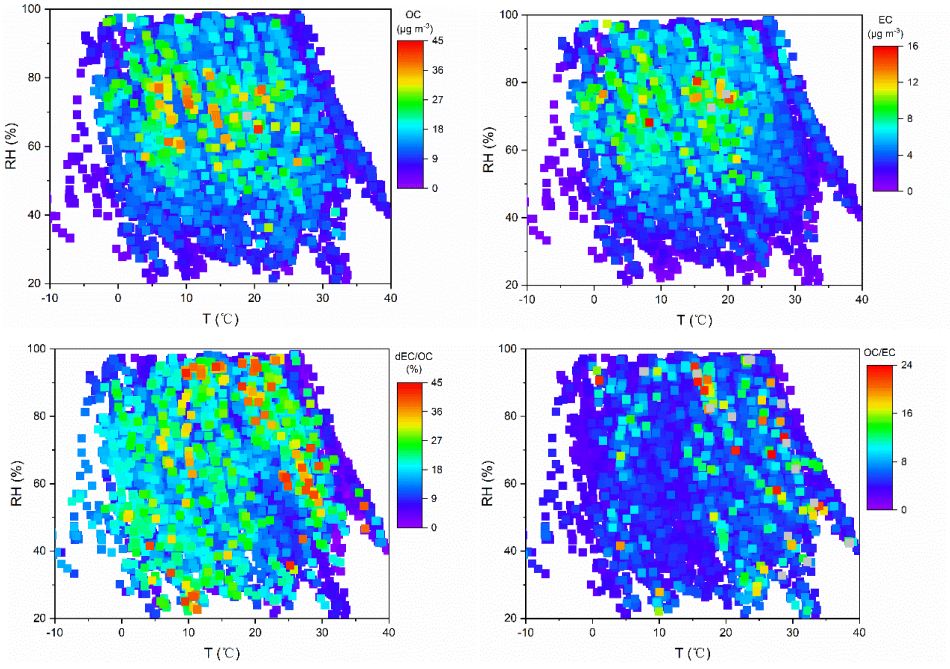

Figure 5. RH/T dependence of OC, EC, dEC/OC and OC/EC ratios during the study periods.

https://doi.org/10.5194/amt-2020-341
Preprint. Discussion started: 9 November 2020

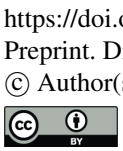

Atmospheric Measurement Techniques Discussions

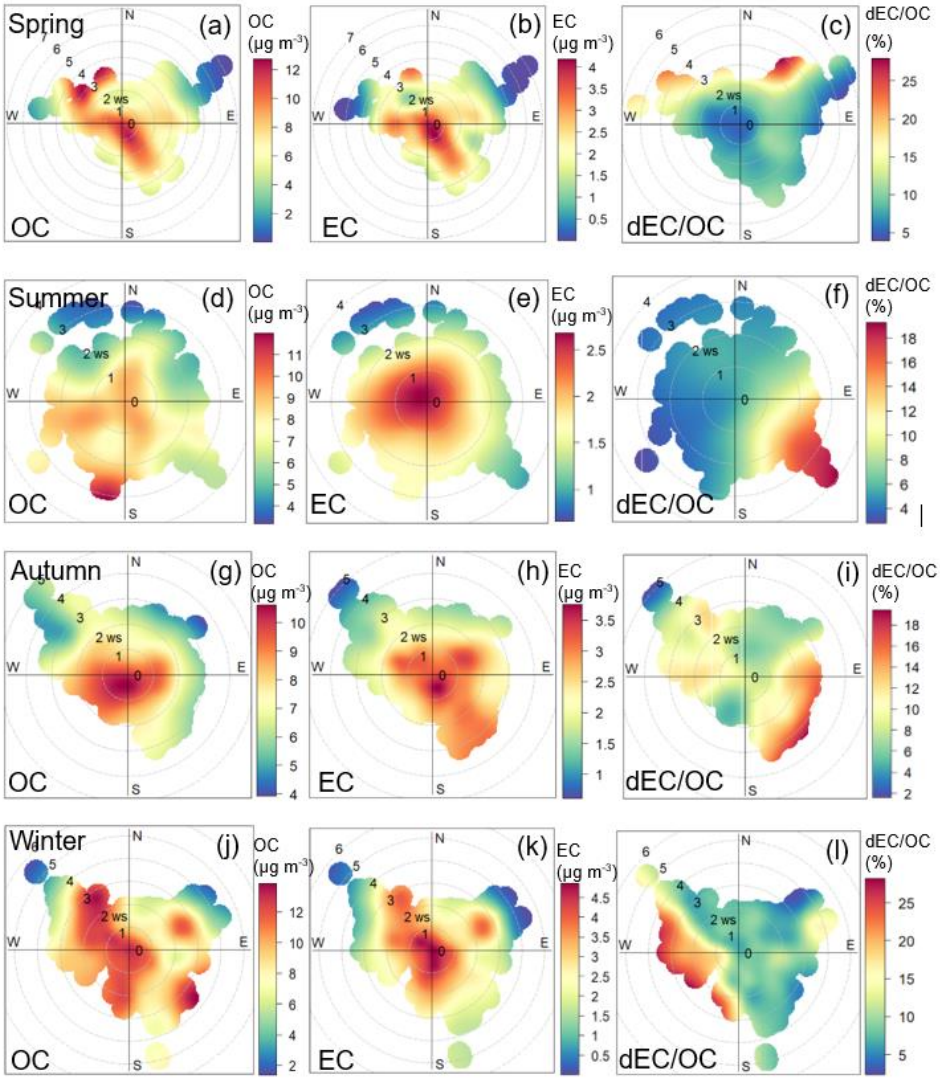

577
578 **Figure 6.** Wind rose of OC, EC and dEC/OC in spring ((a), (b), (c)), summer ((d), (e), (f)), autumn
579 (g), (h), (i)) and winter ((j), (k), (l)).

https://doi.org/10.5194/amt-2020-341
Preprint. Discussion started: 9 November 2020

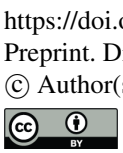

Atmospheric Measurement Techniques Discussions

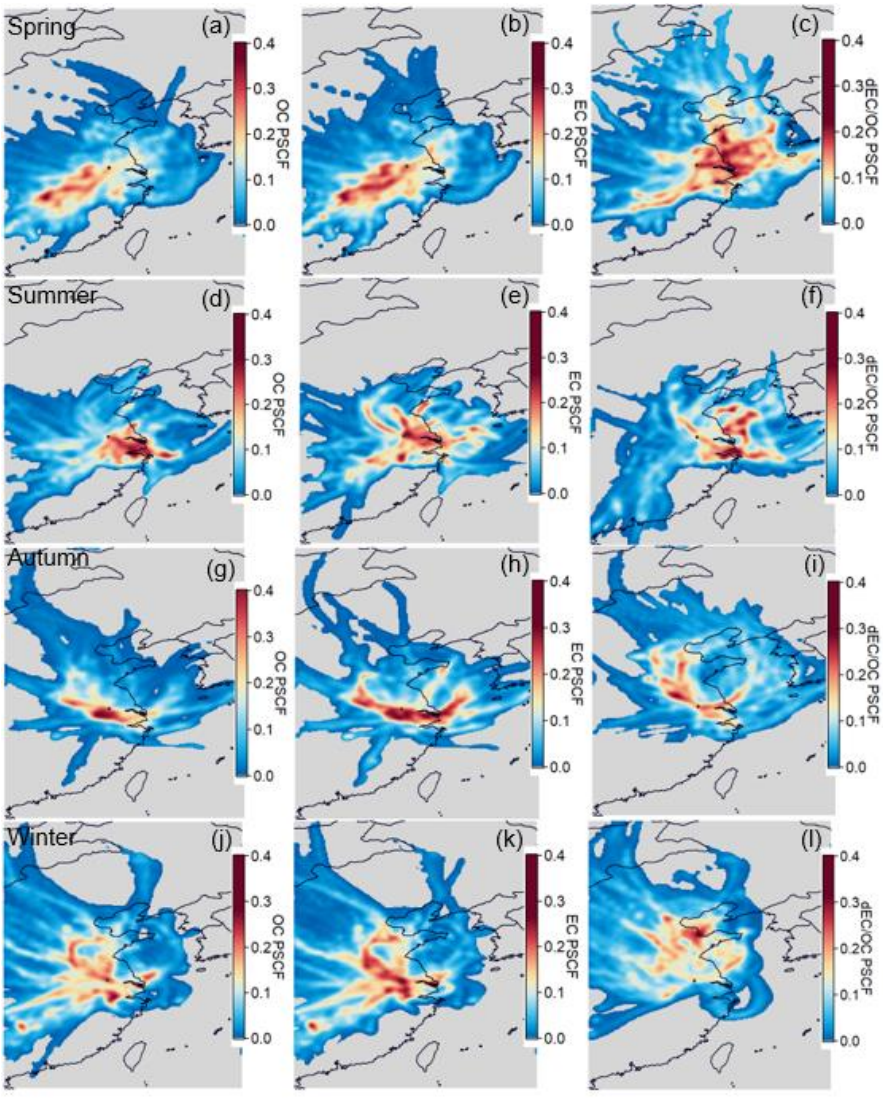

580
581 **Figure 7.** PSCF map for OC, EC and dEC/OC in spring ((a), (b), (c)), summer ((d), (e), (f)), autumn
582 (g), (h), (i)) and winter ((j), (k), (l)).

https://doi.org/10.5194/amt-2020-341
Preprint. Discussion started: 9 November 2020

Atmospheric Measurement Techniques Discussions

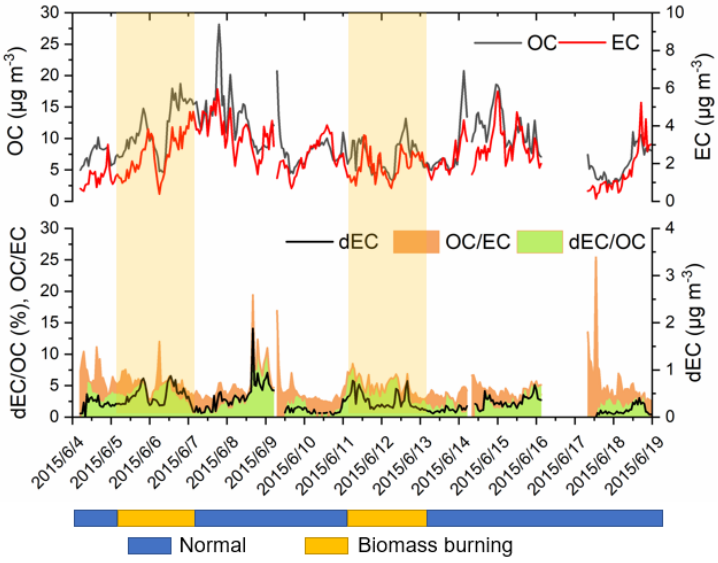

583
584 **Figure 8.** Time series of OC, EC, dEC/OC, dEC and OC/ EC from 4 June 2015 to 19 June 2015.
585 The period was divided into normal days (blue bar) and biomass burning days (yellow bar). The
586 yellow shadow represents the biomass burning periods.

https://doi.org/10.5194/amt-2020-341
Preprint. Discussion started: 9 November 2020

Atmospheric Measurement Techniques Discussions

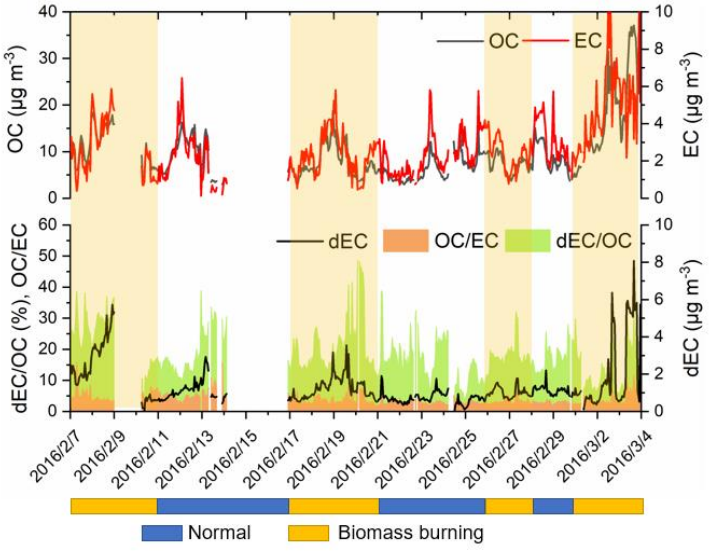

Figure 9. Time series of OC, EC, dEC/OC, dEC and OC/ EC from 7 February 2016 to 3 Mar 2016. The period was divided into normal days (blue bar) and biomass burning days (yellow bar). The yellow shadow represents the biomass burning periods.

https://doi.org/10.5194/amt-2020-341
Preprint. Discussion started: 9 November 2020

Atmospheric Measurement Techniques Discussions

591 **Table 1.** Statistical summary on the $PM_{2.5}$ and carbon species concentrations.

N=5113	Average	Standard Deviation	Media	Min	Max
$PM_{2.5}$ (μg m^{-3})	77.2	48.6	65.0	2.5	458.1
OC (μg m^{-3})	8.9	5.5	7.5	0.5	45.8
EC (μg m^{-3})	3.1	2.0	2.6	0.0	17.6
OC/EC	3.5	2.4	2.9	1.0	29.3
dEC (μg m^{-3})	0.8	0.8	0.6	0.0	8.1
dEC/OC (%)	10.0	7.2	8.6	0.0	48.2
OC/$PM_{2.5}$ (%)	12.8	5.6	11.6	0.7	66.2
EC/$PM_{2.5}$ (%)	4.3	2.3	3.9	0.0	33.2
dEC/$PM_{2.5}$ (%)	1.3	1.2	0.9	0.0	17.6

592

https://doi.org/10.5194/amt-2020-341
Preprint. Discussion started: 9 November 2020

Atmospheric Measurement Techniques Discussions

593 **Table 2.** Statistics of OC, EC, OC/EC, dEC and dEC/OC during biomass burning days and normal
594 days. The values represent average±standard deviation.

		OC ($\mu g\ m^{-3}$)	EC ($\mu g\ m^{-3}$)	OC/EC	dEC ($\mu g\ m^{-3}$)	dEC/OC **(%)**
June 4th to 19th	Normal days	9.5±4.5	2.6±1.3	4.3±2.3	0.2±0.1	2.5±1.3
	Biomass burning days	9.0±3.6	2.0±0.9	4.8±1.6	0.4±0.2	4.6±1.4
February 7th to Mar 3rd	Normal days	7.5±3.3	2.5±1.2	3.3±1.3	0.8±0.3	12.7±5.6
	Biomass burning days	11.2±7.2	3.1±1.9	4.0±1.8	1.7±1.4	15.4±7.8

595
596
597
598